Early Stage Kinetics of Phase-Separating Liquid Mixtures

S. Buil,* J. P. Delville,† and A. Ducasse

Centre de Physique Moléculaire Optique et Hertzienne, UMR CNRS/Université No. 5798, Université Bordeaux I, 351 Cours de la Libération, F-33405 Talence Cedex, France

(Received 27 July 1998)

Observation of the very early stage of phase separation is made difficult by the large number of nucleated domains and the polydispersity of the droplet distribution. We investigate this issue using laser waves to locally quench a liquid mixture with two intersecting pump beams whose interference pattern traps the nuclei on the fringes. The time-resolved reflectivity of a third probe wave on the induced droplet grating (i) confirms that nucleation is heterogeneous even in the bulk, and (ii) surprisingly shows that impurities lead to an unexpected reduction of the growth onto a single "medium-dependent master curve" when samples are synthesized with the same lots of constituents. [S0031-9007(99)08577-4]

PACS numbers: 64.75.z+g, 64.60.Qb, 64.70.Ja, 82.70.Kj

The birth of a new phase in a metastable mixture occurs via nucleation and growth. Even if pioneering works were devoted to nucleation [1], growth processes have been much more investigated [2]. The Ostwald ripening mechanism, i.e., the late stage of droplet growth by evaporation and condensation, is the best known [3,4]. Recently, it has been predicted that Ostwald ripening is preceded by a diffusion-driven free-growth stage $R \propto t^{1/2}$ [15], where R is the droplet radius and t is the time. Experimental investigations [6,7] brought attention back to the starting point of the decay of a metastable state, since they indirectly demonstrated that bulk nucleation in binary liquid mixtures can be heterogeneous. Measurements where then at variance with the usually considered homogeneous nucleation picture [8]. Unfortunately, in previous studies [9], accessible times were not sufficiently early to visually discriminate a prevailing nucleation mechanism. On the other hand, multiple scattering and droplet polydispersity at the early stage generally make inappropriate classical light scattering methods for such an investigation [6], even with thin samples, due to the increasing importance of heterogeneous nucleation [10] and wetting couplings [11] on the boundaries.

Using a wave mixing experiment, we show in this Letter that transient grating techniques circumvent these difficulties. Two interfering pump waves quench locally a binary liquid mixture and confine the transition to the excited bulk area; rigid boundaries play no role. Moreover, the fringes optically trap the nucleated domains in the quenched region. As a consequence, a grating of droplets is generated and their growth can be deduced from the dynamic reflectivity of a third probe beam. This method has two more advantages. The reflectivity is induced by coherent scattering. Thus, as soon as saturation effects can be ignored (as for the early stage kinetics induced by the low supersaturations described here), the reflectivity is proportional to the single-scattering Rayleigh cross section [12] and its time dependence is almost unaffected by multiple scattering. Moreover, since the diffracted wave is related to the induced periodic modulation of the refractive index, the droplet polydispersity does not blur the measurements. A mean growth may therefore be observed.

Experiment.—A schematic of the experiment (detailed in Ref. [13]) is presented in Fig. 1(b). The grating is created from a linearly polarized cw Ar^+ laser in the TEM_{00} mode (wavelength in vacuum: $\lambda_0 = 5145$ Å) whose beam is divided into two parts of equal intensity and path length. These two pump beams are then recombined and intersect in the sample with a definite angle θ. A spatially periodic intensity distribution is built in the sample. For a medium of refractive index n_M, it is characterized by a fringe spacing in the x direction $\Lambda_0 = \lambda_0/2n_M \sin(\theta/2)$ and a spatial wave vector $q_0 = 2\pi/\Lambda_0$. The induced grating is probed by one of the incident write beams which is attenuated and retroreflected back through the sample after a 90° rotation of the polarization. The reflected wave is then extracted with a Glan prism and detected by means of a photon counter connected to a multichannel analyzer.

The experiment was performed in a water-in-oil micellar phase of microemulsion. Our sample (ultrapure water:

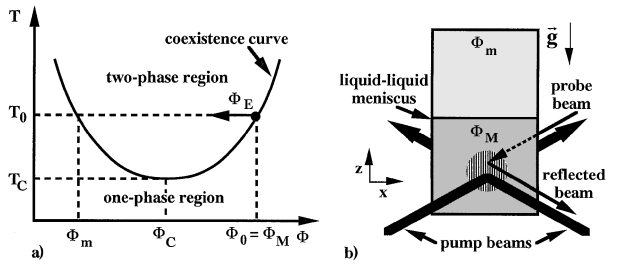

FIG. 1. Schematic phase diagram of the micellar system. Φ_E is the local quench in composition induced by the pump waves; the weak thermal component of the quench has been neglected. Φ_c and T_c are the coordinates of the critical point. (b) Experimental configuration. The grid represents the grating induced in the phase Φ_M.

5%; *n*-dodecane: 78%, *n*-pentanol: 12.2% of spectroscopic quality; crystallized sodium dodecyl sulfate: 4.8%) has a low critical point at a temperature $T_c = 32°\,\mathrm{C}$, above which it phase separates in two micellar phases of different concentrations [Fig. 1(a)]. Since close to T_c they belong to the universality class ($d = 3, n = 1$) of the Ising model, such supramolecular media are particularly interesting to investigate the early stages of phase separation because the amplitude of the correlation length of density fluctuations ξ^- is intrinsically large: In the two-phase region $\xi^- = \xi_0^-|1 - T/T_c|^{-\nu}$ with $\xi_0^- = 11$ Å and $\nu = 0.63$. Moreover, laser waves can easily induce two processes that can modify the micellar composition [14]. The first is electrostriction, but dipolar effects are negligible in the chosen microemulsion [14]. Besides, even if the wavelength λ_0 is off resonance, our mixture is characterized by a very small residual absorption $\alpha_a = 5.58\ 10^{-4}\ \mathrm{cm}^{-1}$. Despite the weakness of the resulting overheating [15], concentration gradients can be induced by thermodiffusion, particularly in near-critical microemulsions for which (i) the Soret constant k_T diverges near the critical point ($k_T = k_T^0|1 - T/T_c|^{-\nu}$) and (ii) k_T is intrinsically large (in our medium $k_T^0 \approx 3$ [15]). Let Φ_0 and T_0 denote the volumic concentration of micelles Φ and temperature T in the absence of a electromagnetic wave and let Φ_E and T_E denote their field intensity variations. Since the thermal diffusivity is much larger than the solute diffusion constant $D^- = k_B T/6\pi\eta\xi^-$, the small overheating can be assumed as almost instantaneous compared to the nucleation time scale. Then, if $I(q)$ is the Fourier component of the intensity distribution for an excited spatial wave vector $q \neq 0$, one obtains [12]

$$T_E(q) = \frac{\alpha_a}{\Lambda_{\mathrm{th}}}\,\frac{I(q)}{q^2}\,, \tag{1a}$$

$$\Phi_E(q,t) = -\frac{\varrho_0}{\varrho_d}\,\frac{k_T}{T_0}\,T_E(q)\left[1 - \exp(-D^- q^2 t)\right], \tag{1b}$$

where η, Λ_{th}, ϱ_0, and ϱ_d are the bulk viscosity, thermal conductivity, and densities of the sample and the micelles.

To observe these field effects, the mixture is enclosed in a temperature-controlled parallelepipedic fused quartz cell (optical path $l = 2$ mm, 1 cm wide). As schematically illustrated in Fig. 1, the temperature T_0 was chosen above T_c (i.e., the sample is in a two-phase equilibrium state). Since $k_T > 0$, a beam power increase from the high micellar concentration phase in coexistence (of concentration $\Phi_M = \Phi_0$) locally quenches the medium in composition in the metastable region; a thermal contribution of the quench should also be added but, practically, it is weak due to the low absorption α_a and the large k_T value. Despite the periodicity of the grating, this quench is essentially driven by the spatial Gaussian intensity distribution of the pump beams, independently of their interference. Indeed, since $\Phi_E(q,t) \propto T_E(q) \propto I(q)/q^2$, the wave vector distribution centered around the $q = 0$ mode associated with each pump beam is always strongly enhanced compared to any particular $q = q_0 \neq 0$ grating mode. This can be illustrated in direct space at the beam intersection ($z = 0$) by writing the inverse Fourier transform of Eqs. (1a) and (1b) as $T_E(x) = T_E^{\bar{q}=0}(x) + T_E^{q=q_0}(x)$ and $\Phi_E(x,t) = \Phi_E^{\bar{q}=0}(x,t) + \Phi_E^{q=q_0}(x,t)$, where $T_E^{\bar{q}=0}(x)$ and $\Phi_E^{\bar{q}=0}(x,t)$ are the pump wave contributions given by [12,15]

$$T_E^{\bar{q}=0}(x) = \frac{\alpha_a P}{4\pi\Lambda_{\mathrm{th}}}\left[-E_1\left(\frac{x^2}{a_0^2}\right) - \ln\left(\frac{x^2}{a_{\mathrm{cl}}^2}\right)\right], \tag{2a}$$

$$\Phi_E^{\bar{q}=0}(x,t) = \frac{\varrho_0}{\varrho_d}\,\frac{k_T}{T_0}\,T_E^{\bar{q}=0}(x)\left[1 - \exp\left(-\frac{D^-}{a_0^2}\,t\right)\right], \tag{2b}$$

where P is the total power injected into the cell and a_0 is the beam radius. The distance a_{cl} is defined by the boundary condition: $T_E^{\bar{q}=0}(x = a_{\mathrm{cl}}) = 0$ and $E_1(x)$ is the one-argument exponential integral function. Typically, using data given in [14], one finds on the axis a stationary supersaturation $|\Phi_E^{\bar{q}=0}(x = 0, t = \infty)|/(\Phi_M - \Phi_m) = 0.13$ for $(T_0 - T_c) = 1.5$ K, $P = 1.2$ W, $a_0 = 23$ μm, and $a_{\mathrm{cl}} = 10a_0$. By comparison, for $\Lambda_0 = 3.5$ μm, the fringe contribution $|\Phi_E^{q=q_0}(x = 0, t = \infty)|(\Phi_M - \Phi_m) = 4.10^{-5}$ to the quench is completely negligible.

Droplets of concentration Φ_m are therefore nucleated by the intensity distribution of each pump beam [15]. Because of the local character of electrostriction [12], these droplets are optically trapped by the fringes (the refractive index of Φ_m is larger than that of Φ_m because the refractive index of water is slightly smaller than that of *n*-dodecane) and thus grow in the quenched region. To observe the very early stage kinetics of the transition, a three-step experimental procedure is implemented: (i) At $t = 0$, the two pump beams simultaneously quench the mixture; a grating of growing droplets is generated; (ii) At $t = t_1$, one pump wave is obturated to observe the grating relaxation during $t_2 - t_1$; (iii) At $t = t_2$, both pump beams are obturated till t_3 $[(t_3 - t_2) \approx 5t_1)]$ to ensure a thermodynamic relaxation of the system before starting a new accumulation.

Results.—Let $\varphi_D(t)$ represent the field variation of the volumic concentration of nucleated droplets. Then, as for a liquid suspension of dielectric spheres [16], the dynamic reflectivity $\mathrm{Re}(t)$ (ratio of the diffracted to the incident probe beam intensities) behaves as $\mathrm{Re}(t) \propto |\varphi_D(t)|^2$. An example is given in Fig. 2 for four different t_1. Let us first consider the grating relaxation. Since one pump beam is obturated at $t = t_1$, a "reverse quench" [9], still within the two-phase region, is induced in the system. Thus, the growth instantly slows down, and it can be assumed that the grating relaxes faster than the droplet radius evolves. Therefore,

$$\mathrm{Re}(t > t_1) \propto \exp[-2D_R(t_1)q_0^2(t - t_1)], \tag{3}$$

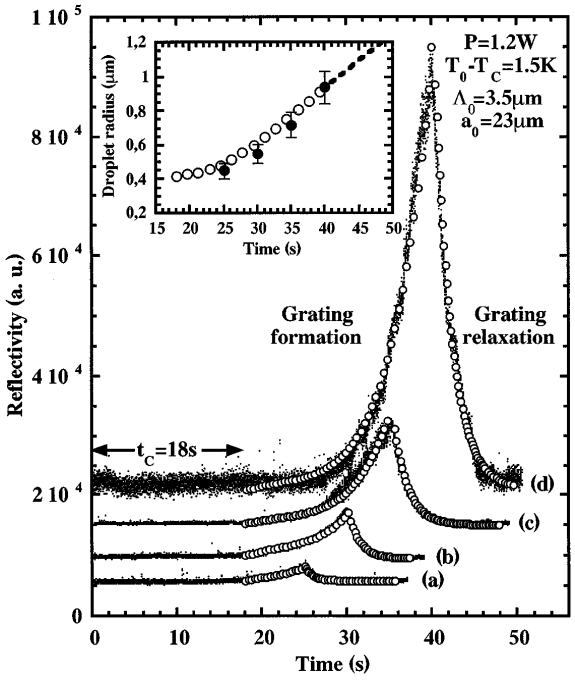

FIG. 2. Reflectivity of the probe beam induced by the formation and the relaxation of a droplet grating when one pump wave is obturated at (*a*) $t_1 = 25$ s, (*b*) $t_1 = 30$ s, (*c*) $t_1 = 35$ s and (*d*) $t_1 = 40$ s. The fits (empty circles) are performed according to Eqs. (3) and (4). Inset: droplet growth law (empty circles) deduced from the fit of the grating formations. The filled circles are the radii at t_1 deduced from the grating relaxations. The dashed line shows the continuation of the growth which was not measured.

where $D_R(t) = k_B T/6\pi\eta R(t)$. From Fig. 2, we deduce $R(t_1 = 25\ \mathrm{s}) = 0.45\ \mu$m, $R(t_1 = 30\ \mathrm{s}) = 0.55\ \mu$m, $R(t_1 = 35\ \mathrm{s}) = 0.72\ \mu$m, and $R(t_1 = 40\ \mathrm{s}) = 0.94\ \mu$m. On the other hand, it can be observed on grating formations that the reflectivities start to increase after an illumination time $t \approx 20$ s (an accurate determination is given below). Thus, if nucleation is homogeneous, the critical radius should be of the order of $(\xi^-/3)|(\Phi_M - \Phi_m)/(\Phi_E^{\bar{q}=0}(x = 0, t = 20\ \mathrm{s})| = 1\ \mu$m, a value larger than the different $R(t_1)$ measured for longer illumination times. As already discussed [6,7], this comparison suggests that nucleation is heterogeneous in mixtures, a phenomenon which seems unavoidable since here the transition is strictly induced in the bulk. To confirm this fact, let t_c and $\Delta_E(x = 0,\ t = t_c)$ denote the mean time and supersaturation needed to initiate heterogeneous nucleation. Then, the grating formation for $t_c < t < t_1$ is described by

$$\mathrm{Re}(t_c < t < t_1) \propto |\varphi_D(t)|^2, \tag{4a}$$

$$\frac{\partial \varphi_D}{\partial t} = -D_R(t) q_0^2 [\varphi_D(t) + \mathrm{AR}(t)^3 I(q_0)], \tag{4b}$$

$$\frac{\partial R}{\partial t} = \frac{D^- \Delta_E(x = 0, t = t_c)}{R(t)} \left(1 - \frac{R_c}{R(t)}\right). \tag{4c}$$

Equation (4b) simply describes the diffusion-driven optical manipulation of the droplets by the fringes; $AR(t)^3$ is proportional to droplet polarizability. Since nucleation is supposed to be heterogeneous, a majority of droplets are nucleated on a finite number of seeds corresponding to the bulk impurities. On the other hand, Eq. (4c) corresponds to the familiar growth rate of an isolated droplet because finite size effects induced by the pump beam radii [15] are completely negligible at this stage; $R_c = \xi^-/3\Delta_E(x = 0, t = t_c)$ is the heterogeneous critical radius [6]. To obtain an accurate description of the very early stage growth, i.e., of the quantities t_c and $\Delta_E(x = 0, t = t_c)$, the grating formation for the whole set of runs (four in the case of Fig. 2) is fitted together. The initial conditions for solving Eqs. (4b) and (4c) are, respectively, $\varphi_D(t_c) = 0$ and $R(t_c) = R_c + \xi^-/2$, where $\xi^-/2$ corresponds to an uncertainty on the activation energy of the order of $k_B T$[8]. From the experiment in Fig. 2, we get $t_c = 18 \pm 1$ s and $\Delta_E(x = 0, t = t_c) = 0.026 \pm 0.003$. The resulting droplet growth at the very early stage is shown in the inset of Fig. 2. A good agreement is observed between the kinetics obtained from the fit of the grating formations and the droplet radii measured at t_1 from the associated relaxations. Since the relative error on the beam power is $dP/P \leq 5\%$ and the temperature is regulated at better than 0.05 K, we deduce $d\Delta_E/\Delta_E \leq 10\%$. Then, assuming $dR/R \approx dR_c/R_c$, we may expect $dR/R \leq 7\%$, in agreement with the experiments. Moreover, since $D^- t_c/a_0^2 \ll 1$, we estimate $dt_c/t_c \leq 13\%$ from Eq. (2b). In fact, by using t_c and Δ_E given by the fits, the reflectivities are recovered only with a smaller uncertainty: $dt_c/t_c \leq 5\%$. Finally, despite the agreement observed in Fig. 2, we also tried to fit the data, without any success, considering a nucleation rate at the early stage [8]. The slope of the observed grating formations is too weak to integrate the resulting increase in droplet density and eliminates definitively a homogeneous nucleation process.

Discussion.—If the reduced variables $\varrho = R/R_c$ and $\tau = D^- \xi^-/3R_c^3(t - t_c)$ are considered, Eq. (4c) can be written in a universal form: $\partial\varrho/\partial\tau = (\varrho - 1)/\varrho^2$ whose integration leads to

$$\tau = K + \ln(\varrho - 1) + \varrho + \varrho^2/2, \tag{5}$$

where K is a constant that characterizes the nucleation conditions. Since small variations in K (such as those driven by thermodynamic fluctuations for homogeneous nucleation) are able to induce huge modifications in early stage growth [6], it is usually accepted that this K dependence eliminates the existence of any universal behavior as long as the condition $\varrho \gg 1$ is not satisfied. However, as soon as their mean size is larger than ξ^-, impurities are known to strongly decrease the activation barrier and to dampen the influence of thermodynamic fluctuations on nucleation. We can then make the hypothesis that K essentially depends on the properties of the fixed number of heterogeneous seeds that are preferentially wetted by

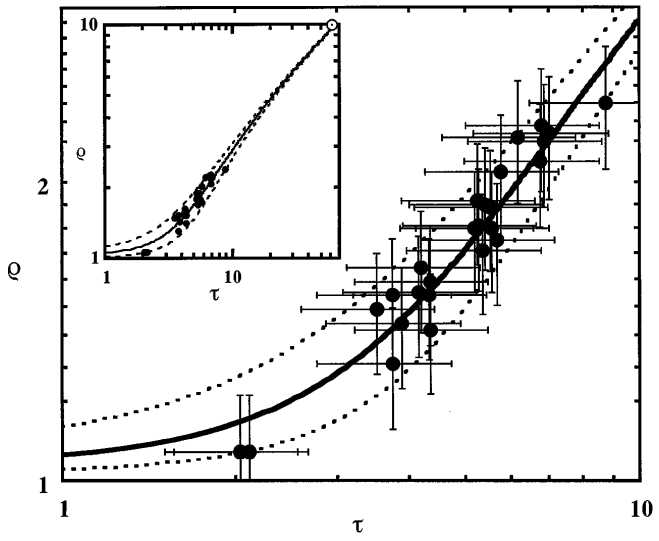

FIG. 3. Plot in reduced variables of the radii at t_1 obtained for ten different experiments (filled circles). The solid line represents a fit performed with Eq. (5). The two surrounding dashed curves illustrate the evolution of the largest measured growth law dispersion towards the universal free-growth regime $R \propto t^{1/2}$. An overview is presented in the inset, which also shows the location of the earliest free-growth measurement (empty circle) given in Ref. [7].

the minority phase. A simple rescaling of a set of experiments done in different samples (made with the same lots of constituents and therefore with the same type and quantity of impurities) and for different values of the control parameters $(P, a_0, \Lambda_0, T_0 - T_c)$ should therefore point out a single-scaled dynamics of the early stage droplet growth. This data rescaling is shown in Fig. 3 for ten experiments (including that of Fig. 2) made in eight different samples and describing a reasonably wide region of the parameter space: $0.6 \leq P \leq 1.2$ W, $12 \leq a_0 \leq 32$ μm, $\Lambda_0 = 3.5$ μm, and $0.7 \leq T_0 - T_c \leq 2$ K. The dots represent, during slightly less than one decade in reduced time $(2 \leq \tau \leq 9)$, the different couples $[R(t_1), t_1 - t_c]$ deduced from the grating relaxations. Using the estimations given above, errors are $d\varrho/\varrho \leq 14\%$ and $d\tau/\tau \leq 26\%$. Over time scales much smaller than any of those already investigated ($\tau \geq 60$ in simple fluid mixtures [7] and $\tau \geq 80$ in polymer blends [6]), all of the data are closely distributed around a mean growth behavior illustrated by the solid line. The fit from Eq. (5) gives $K = 2.15 \pm 0.1$. As a consequence, for $T_0 - T_c \geq 0.7$ K (i.e., for $\xi^- \leq 0.05$ μm), the rescaling illustrates that the mean seed size behaves as a particular length scale which, as expected, almost nulifies the influence of thermodynamic fluctuations. Moreover, unlike the usually accepted idea that heterogeneous nucleation is too versatile to be quantified, Fig. 3 shows, surprisingly, that the data follow the same reduced law in the presence of bulk impurities. Thus, for the same lots of components, as soon as the decay of a metastable state has been characterized once to get the K value, the kinetics becomes completely predictable. This conclusion, which obviously deserves further investigation in other systems, could have important technological significance in material science, particularly for microcrystalline formation in doped glasses [17].

Finally, as observed in previous studies at larger τ [6], and partly illustrated by the largest dispersion of our measurements [the lower ($K_{\max} = 3.1$) and the higher ($K_{\min} = 1.25$) dashed lines in Fig. 3], the early stage kinetics develops towards the universal free-growth regime $R \propto t^{1/2}$, regardless of the initial conditions. Therefore, the agreement between measurements made for $\tau \geq 60$ in Ref. [7] [the earliest datum ($\varrho = 10$, $\tau = 60$) is shown in the inset of Fig. 3 for the sake of comparison] with our fitting curve illustrates over four decades in time (from $\tau = 2$ to $\tau = 2 \times 10^4$ [16]) the global evolution of the dynamics of phase-separating liquid mixtures from the very early stage to the free-growth regime.

We are grateful to E. Freysz and Y. Garrabos for helpful discussions, and to J. Plantard and M. Winckert for technical assistance. This work was partly supported by the Région Aquitaine.

*Email address: buil@frbdx11.cribx1.u-bordeaux.fr
†Email address: delville@frbdx11.cribx1.u-bordeaux.fr

[1] J. W. Gibbs, *The Scientific Papers of J. W. Gibbs* (Dover, New York, 1961).
[2] J. D. Gunton, M. San Miguel, and P. S. Sahni in *Phase Transition and Critical Phenomena,* edited by C. Domb and J. L. Lebowitz (Academic, New York, 1983), Vol. 8.
[3] I. M. Lifshitz and V. V. Sloyzov, J. Phys. Chem. Solids **19**, 35 (1961).
[4] N. Akaiwa and P. W. Voorhees, Phys. Rev. E **49**, 3860 (1994), and references therein.
[5] M. Tokuyama and Y. Enomoto, Phys. Rev. Lett. **69**, 312 (1992).
[6] A. Cumming *et al.,* Phys. Rev. Lett. **65**, 863 (1990); Phys. Rev. A **45**, 885 (1992).
[7] T. Baumberger *et al.,* Phys. Rev. A **46**, 7636 (1992).
[8] J. S. Langer and A. J. Schwartz, Phys. Rev. A **21**, 948 (1980).
[9] E. D. Siebert and C. M. Knobler, Phys. Rev. Lett. **52**, 1133 (1984).
[10] D. Beysens *et al.,* Phase Transit. **31**, 219 (1991).
[11] J. Bodensohn and W. I. Goldburg, Phys. Rev. A **46**, 5084 (1992).
[12] E. Freysz *et al.,* Phys. Rev. E **49**, 2141 (1994).
[13] S. Buil *et al.,* Opt. Lett. **23**, 1334 (1998).
[14] J. P. Delville *et al.,* Phys. Rev. E **49**, 4145 (1994).
[15] C. Lalaude *et al.,* Phys. Rev. Lett. **78**, 2156 (1997).
[16] P. W. Smith *et al.,* Opt. Lett. **7**, 347 (1982).
[17] C. Flytzanis *et al.,* Prog. Opt. **29**, 323 (1991).